Neurobiology of Aging 117 (2022) 117–127

Contents lists available at ScienceDirect

Neurobiology of Aging

journal homepage: www.elsevier.com/locate/neuaging.org

Structural covariance changes in major cortico-basal ganglia and thalamic networks in amyloid-positive patients with white matter hyperintensities

Sang Joon Son[a], Chang Hyung Hong[a], Na-Rae Kim[a], Jin Wook Choi[b], Hyun Woong Roh[a], Heirim Lee[c,d], Sang Won Seo[e], Seong Hye Choi[f], Eun-Joo Kim[g], Byeong C. Kim[h], Seong Yoon Kim[i], Jaeyoun Cheong[j], So Young Moon[k], Bumhee Park[c,d,*]

[a] Department of Psychiatry, Ajou University School of Medicine, Suwon, Republic of Korea
[b] Department of Radiology, Ajou University School of Medicine, Suwon, Republic of Korea
[c] Department of Biomedical Informatics, Ajou University School of Medicine, Suwon, Republic of Korea
[d] Office of Biostatistics, Medical Research Collaborating Center, Ajou Research Institute for innovative Medicine, Ajou University Medical Center, Suwon, Republic of Korea
[e] Department of Neurology, Samsung Medical Center, Sungkyunkwan University School of Medicine, Seoul, Republic of Korea
[f] Department of Neurology, Inha University School of Medicine, Incheon, Republic of Korea
[g] Department of Neurology, Pusan National University School of Medicine, Pusan, Republic of Korea
[h] Department of Neurology, Chonnam National University School of Medicine, Gwangju, Republic of Korea
[i] Department of Psychiatry, Asan Medical Center, University of Ulsan College of Medicine, Seoul, Republic of Korea
[j] Human Genome Research and Bio-Resource Center, Ajou University Medical Center, Suwon, Republic of Korea
[k] Department of Neurology, Ajou University School of Medicine, Suwon, Republic of Korea

ARTICLE INFO

Article history:
Received 28 July 2020
Revised 19 May 2022
Accepted 23 May 2022
Available online 27 May 2022

Keywords:
Structural covariance network
Amyloid
White matter hyperintensities

ABSTRACT

Synergistic effects of amyloid deposition and cerebral small vessel disease (CSVD) on the systematic disruption of large-scale brain anatomical organization are not well known. We investigated the brain structural covariance network (SCN) in 245 cognitively impaired older adults with the information of amyloid deposition and CSVD represented by white matter hyperintensities (WMH). We stratified the participants into 4 groups based on amyloid burden (A+/A -) and WMH severity (W+/W-). Using source-based morphometry analysis, we selected 13 independent components (ICs) in functional brain networks. SCNs between ICs were defined using Pearson correlations between individual weights; SCNs of the A+W+ group were compared with those of other groups using Fisher's r-to-z transformation. Our results revealed that SCN characteristics related to amyloid burden with CSVD could be represented by decreased intra- and increased cortico-subcortical inter-network connectivity in the salience (SN) and default mode networks (DMN), decreased cortico-subcortical internetwork connectivity in the central executive network (CEN), and altered internetwork connectivity among DMN-SN-CEN. Amyloid deposition and CSVD maybe associated with altered connectivity in structural networks in the brain and should be considered when assessing network disruption.

1. Introduction

Organization patterns of brain structure varies between people and clusters of brain regions co-vary in their morphological properties. The brain volume in 1 region may influence volume

We certify that the attached manuscript describes properly conducted and documented original research. All authors have reviewed the contents of the manuscript being submitted, approve of its contents and validate the accuracy of the data. There are no conflicts of interest to declare. The attached manuscript has not been submitted to or published by any other journal, and it will not be submitted to any other journal before the final decision has been taken as to its acceptability by Neurobiology of Aging.

* Corresponding author at: Department of Biomedical Informatics, Ajou University School of Medicine, Suwon 16499, Republic of Korea. Phone number: +82-31-219-4458 Fax number: +82-31-219-4472
E-mail address: bhpark@ajou.ac.kr (B. Park).

0197-4580/$ – see front matter
https://doi.org/10.1016/j.neurobiolaging.2022.05.010

changes in other structurally and functionally connected regions (Alexander-Bloch et al., 2013a; Hoagey et al., 2019; Spreng et al., 2019). Such structural networks are thought to be shaped by genetic and environmental influences (Richmond et al., 2016) and may continue to be reshaped during their lifespan (Aboud et al., 2019; Alexander-Bloch et al., 2013b) by various trophic influences (Mechelli, 2005; Yun et al., 2020). Structural covariance network (SCN) analysis is a standard approach for mapping the large-scale network architecture of anatomically connected regions in the human brain (Evans, 2013; Seidlitz et al., 2018). Interestingly, SCNs tend to be similar to patterns of functional connectivity (Soriano-Mas et al., 2013), suggesting that it may reflect the connectivity of functional networks and help identify foci of gray matter loss in neurodegenerative diseases (Alexander-Bloch et al., 2013a; Seeley et al., 2009).

Alzheimer's disease (AD) is the most common cause of dementia worldwide but, the underlying etiologies and pathophysiology of AD are not yet fully understood, and there is currently no effective treatment for AD (Winblad et al., 2016). Researchers have suggested that a mixed pathology involving vasculopathy or other proteinopathies may be a possible reason (Brenowitz et al., 2017; Kapasi et al., 2017) for the disappointing outcomes of disease modifying AD trials (Doody et al., 2014; Hardy and De Strooper, 2017; Schneider, 2020). Recent studies have shown that along with cerebral vascular disease markers, the presence of amyloid deposition, a hallmark of AD, is also frequently observed in patients with vascular cognitive impairment (Chui et al., 2006; Ye et al., 2015). This strongly suggests that progressive cognitive decline in patients with cerebral small vessel disease (CSVD) is primarily driven by the amyloid burden or synergistic effects of amyloid and vascular burdens (Chui et al., 2006; Ye et al., 2015). Therefore, investigating the effects of amyloid deposition on brain architectural changes in the presence of CSVD is an important research goal.

Several studies have reported selective disruption of cortical and subcortical structural hub networks in AD and CSVD separately (Foster-Dingley et al., 2016; Montembeault et al., 2016; Nestor et al., 2017). However, the combined effects of amyloid deposition and CSVD on the systematic disruption of large-scale brain anatomical networks are not well known. We hypothesized that there would be unique SCN patterns when these 2 pathologies coexist. Thus, we investigated altered SCNs related to amyloid deposition accompanied by CSVD in older adults with cognitive impairment using the standard uptake value ratio (SUVR) of amyloid positron emission tomography (PET) and white matter hyperintensities (WMH) on brain magnetic resonance imaging (MRI) data, which are known to be associated with accelerated cognitive decline and amyloid deposition among the CSVD markers (Ye et al., 2015).

2. Materials and methods

2.1. Participants

This study was a part of the ongoing Biobank innovations for chronic cerebrovascular disease with Alzheimer's disease study (BICWALZS) undertaken by the Center for Convergence Research of Neurological Disorders. BICWALZS was planned and initiated in October 2016 by the Korea Disease Control and Prevention Agency for the Korea Biobank Project, which is a national innovative biobanking program that fosters biomedical and healthcare research and development infrastructure. The memory clinics of 5 university hospitals (Ajou University Hospital, Samsung Medical Center, Inha University Hospital, Pusan National University Hospital, and Chonnam National University Hospital) and a community geriatric mental health center (Suwon Geriatric Mental Health Center) were involved in this study. Participants were recruited voluntarily from those who visited the neurology or psychiatry memory outpatient clinics. The original goal was to facilitate, regulate, and ensure optimal use of human biological specimens for research in the fields of subjective cognitive decline (SCD), mild cognitive impairment (MCI), AD, and subcortical vascular dementia (SVaD). The BICWALZS is registered with the Korean National Clinical Trial Registry, Clinical Research Information Service (identifier: KCT0003391). This study was approved by the Institutional Review Board of Ajou University Hospital (AJIRB-BMR-SUR-16-362). Written informed consent was obtained from all participants and caregivers.

We analyzed data from 245 patients with available amyloid deposition and WMH severity information from amyloid PET, 3DT1, and T2 fluid-attenuated inversion recovery (FLAIR) MRI data. An overview of the inclusion/exclusion criteria for participants and a flow chart of the sample derivation are presented in supplementary table 1. The clinical diagnosis criteria used for this study were as follows: SCD criteria included self and/or informant reports of cognitive decline but no impairment in performing objective cognitive tasks. Patients with MCI were evaluated based on a Clinical Dementia Rating (CDR) (Morris, 1993) score of 0.5, and the expanded Mayo Clinic criteria (Winblad et al., 2004). Patients with AD dementia were evaluated using the National Institute on Aging-Alzheimer's Association core clinical probable AD dementia criteria (McKhann et al., 2011). Patients who had above-moderate WMH on MRI while also satisfying the AD dementia criteria were diagnosed as having AD with CSVD. SVaD was evaluated based on above-moderate WMH and vascular dementia criteria in accordance with the Diagnostic Statistical Manual of Mental Disorders, fifth edition (American Psychiatric Association, 2013). We excluded patients with at least 1 of the following criteria: (1) possible frontotemporal lobar degeneration, (2) possible Lewy body dementia, and (3) history of neurological or medical conditions such as territorial cerebral infarction, intracranial hemorrhage, Parkinson's disease, heart failure, renal failure, or others that could interfere with the study.

2.2. Cognitive function assessment and APOE genotyping

Cognitive function was evaluated using the Seoul Neuropsychological Screening Battery (SNSB), which includes standardized neuropsychological tests for language, visuospatial abilities, memory, and frontal/executive function. General cognition, dementia severity, attention ability language function, and visuospatial function were evaluated using the mini-mental state examination, CDR sum of box (CDRSB) score, backwards digit span test, Boston naming test, and Rey complex figure test (RCFT) copy, respectively. Memory function was calculated by adding the scores of verbal memory tests (Seoul verbal learning test -delayed recall and recognition) and visual memory tests (RCFT-delayed recall). Frontal/executive function was calculated by adding the scores of the controlled oral word association test-animal and Stroop test-color reading. Depressive symptoms were evaluated using the Korean version of the short form geriatric depression scale (Ahn et al., 2010). SNSB was validated with norms based on the analysis of 447 healthy subjects, and we used z-scores of each test adjusted for age, sex, and education level (Kang, 2003).

Informed consent for collection and genotyping of blood genomic DNA samples was obtained from all participants. Genomic DNA was isolated from the blood samples, and single-nucleotide polymorphism genotyping was performed using DNA Link (Seoul, Korea) using Affymetrix Axiom KORV1.0-96 Array (Thermo Fisher Scientific, Waltham, MA, USA) according to the manufacturer's pro-

tocol. APOE genotypes were derived from rs429358 and rs7412, which were included in the array.

2.3. Amyloid PET acquisition and measurement of amyloid deposition

The participants underwent ^{18}F-flutemetamol PET scan using a previously published protocol (Roh et al., 2020). The amyloid PET parameters according to the study site are described in Supplementary Table 2. ^{18}F-flutemetamol was injected into the antecubital vein as a bolus (mean dose, 185 MBq). A 20-min PET scan (4 × 5 minute dynamic frames) was performed 90-minute after the injection. ^{18}F-flutemetamol PET scans were co-registered to individual MRI scans, which were normalized to a T1-weighted MRI template using transformation parameters. To quantify ^{18}F-flutemetamol retention, SUVR was obtained using the pons as a reference region. Global cortical ^{18}F-flutemetamol retention was calculated from the volume-weighted average SUVRs of 28 bilateral cortical volumes of interest from the frontal, posterior cingulate, lateral temporal, parietal, and occipital lobes using the automated anatomical labeling (AAL) atlas (Tzourio-Mazoyer et al., 2002). Based on a previous report in the elderly Korean population and the distribution of our data, participants were diagnosed as positive for amyloid deposition if their global cortical SUVR was greater than 0.65 (Bucci et al., 2021; Hwang et al., 2019).

2.4. MRI acquisition and measurement of WMH severity

MRI scan data were obtained from all participants using a 3.0 T MR scanner and previously published protocols (Roh et al., 2020). Structural MRIs, including 3DT1and FLAIR were obtained. All MRI images were reviewed by neuroradiologists. The detailed MRI parameters by site are described in Supplementary Table 3.

FLAIR images were used to evaluate WMH degrees according to the modified criteria proposed by Fazekas et al. (Fazekas et al., 1987) and Scheltens et al. (Scheltens et al., 1993). WMHs were separately examined in periventricular white matter and deep white matter lesions. Deep white matter lesion severity was scored on a 3 -point scale with scores of 1, 2, and 3 corresponding to lesion diameters of less than 10 mm, 25 mm, and greater than 25 mm. Periventricular white matter lesion severity was scored based on the size of the cap and band as, 1 (cap and band <5 mm), 2 (cap and band between 5 mm and 10 mm), or score 3 (cap and band >10 mm), where the cap and band were perpendicular to and horizontal to the ventricle, respectively. The degree of overall WMH was classified as mild or less (D1P1 and D1P2), moderate (D1P3, D2P1, D2P2, D2P3, D3P1, D3P2), or severe (D3P3) based on the severity of periventricular (P) and deep (D) white matter hyperintensity (Noh et al., 2014). The visual rating of WMH was measured by 1 neurologist or psychiatrist at each recruitment site, and the inter-rater reliability of the CREDOS WMH visual rating scale was high (k = 0.726–0.905).

The quantitative WMH volume was also measured using the segmentation module of a commercial software (NordicICE, NordicNeuroLab, Bergen, Norway). The region of interest (ROI)-limited segmentation was automatically performed, in which a polygonal or freehand ROI was drawn roughly with a polygonal or freehand function on a hyperintense lesion in T2 FLAIR MRI, and the correct ROI was generated using a pixel thresholding function by a neuroradiologist (JWC). Volume was calculated as the total hyperintense area in single slices multiplied by the slice thickness. Periventricular WMHs were defined as T2 FLAIR signal alterations in direct contact with the ventricular system. Deep WMHs were defined as T2 FLAIR signal alterations distant from the ventricular system.

2.5. Group stratification based on cortical amyloid burden and WMH severity

Among the BICWALZS participants, 245 subjects identified using both visual and quantitative measurements were selected to evaluate WMH severity in more detail. First, the visual rating of WMH degrees was conducted using the modified criteria mentioned above. Participants with moderate/severe WMH burdens were defined as W+, and those with mild or less WMH burden were defined as W-. Following this, W+ and W- patients, whose quantitative severity scores were below and above the 95th percentile, respectively, were excluded after accounting for age and sex. (Ryu et al., 2014). We stratified the participants into 4 groups based on cortical amyloid burden and WMH severity, irrespective of the clinical diagnosis (amyloid PET positive with moderate/severe WMH: A+W+; amyloid PET positive without moderate/severe WMH: A+W-; amyloid PET negative with moderate/severe WMH: A-W+; amyloid PET negative without moderate/severe WMH: A-W-).te/severe WMH: A-W+; amyloid PET negative without moderate/severe WMH: A-W-).

2.6. Group-wise comparison of demographic, neuropsychological characteristics, and regional gray matter volume

Chi-square and analysis of variance (ANOVA) were used to compare the clinical characteristics among the groups. Regarding the comparison of regional gray matter volume, ANOVA and post-hoc tests corrected using Bonferroni method for multiple comparisons were conducted after controlling for age, sex, total intracranial volume, education years, and multiple sites.

2.7. Source-based morphometry analysis

In this study, we aimed to estimate spatially independent components, rather than single voxel changes, as common patterns of change in gray matter concentration (i.e., covarying brain atrophy). For this purpose, we applied a cross-sectional independent component analysis (ICA) to data preprocessed using voxel-based morphometry (VBM). This method is known as the source-based morphometry (SBM) approach, which can extract spatially independent sources representing covarying multivariate patterns of gray matter volumes between subjects, while the univariate VBM approach can only detect specific group effects at each voxel separately (Xu et al., 2009). In addition, SBM can improve sensitivity by separating several noise effects from true independent sources and reducing multiple comparisons over a large number of voxels (Xu et al., 2009). Due to these advantages, SBM has often been applied in recent neuroimaging studies (Cacciaglia et al., 2020; Duan et al., 2021; Kakeda et al., 2020).

Prior to SBM analysis however, VBM analysis was performed using the SPM12 VBM-Diffeomorphic Anatomical Registration Through Exponentiated Lie Algebra (DARTEL) procedure (SPM12, http://www.fil.ion.ucl.ac.uk/spm/, Wellcome Trust Centre for Neuroimaging, London, UK) (Ashburner, 2007; Ashburner and Friston, 2000; "SPM - Statistical Parametric Mapping," n.d.). A well-trained physician detected no abnormalities due to motion and/or other artifacts on T1-weighted images. T1-weighted image preprocessing included (i) gray matter segmentation based on a standard tissue probability map provided by SPM, (ii) creation of a study-specific template, spatial normalization of individual images to the DARTEL template using DARTEL, and modulation to adjust for volume signal changes during spatial normalization, and (iii) spatial smoothing of the gray matter partitions using a Gaussian kernel of 6 mm full-width at half maximum. In this study, we did not in-

clude the cerebellum as MRI data from some individuals did not fully cover all cerebellar voxels.

To guarantee the reliability of independent sources, we applied the FastICA + ICASSO framework (Himberg et al., 2004, Hyvärinen, 1999; https://research.ics.aalto.fi/ica/fastica/ and https://research.ics.aalto.fi/ica/icasso/) on the VBM-preprocessed data. Specifically, we first reduced the original cross-sectional data of the 245 participants to 84 principal components, where the optimal number of components were determined using Laplace principal component analysis (Beckmann and Smith, 2004). We then ran FastICA on the reduced data 100 times using random initial values (Himberg et al., 2004)(Hyvärinen, 1999). From the pool of independent components (ICs) estimated at each run, ICASSO sought cluster centroids by computing hierarchical clustering according to the dissimilarities among ICs using an average-linkage strategy; these cluster centroids were considered reliable ICs. The hierarchical clustering strategy was performed under the default setting provided in the ICASSO software, and it has been widely used in previous studies (Beckmann and Smith, 2004; Himberg et al., 2004; Hyvärinen, 1999; Murley et al., 2020). SCNs are known to have similar patterns of functional connectivity (Soriano-Mas et al., 2013). Thus, meaningful IC maps were visually identified if they were principally located in gray matter regions and highly stable (reliability >0.8) in the ICASSO results. Among them, we selected the IC maps that were localized at hypothesized large-scale functional brain networks related to AD and CSVD (the default mode network [DMN], central executive network [CEN], salience network [SN], sensorimotor network [SMN], thalamus [THL], and basal ganglia [BG] network) (Montembeault et al., 2016; Nestor et al., 2017). These procedures are shown in Fig. 1A. All group-level IC maps were z-scored and thresholded with z>3 for visualization purposes. To avoid the ambiguity of each terminology, we referred to individual IC maps as structural covariance networks and called connectivity between them, network connectivity in this study.

2.8. Structural covariance network analysis

Network connectivity among the selected ICs was defined using Pearson correlations between individual IC weights. IC weights were defined as values in the loading matrix; each row represents the contribution scores of all ICs to the corresponding subject, and each column of the loading matrix represents how an IC contributes to all subjects differently. We regressed out the effects of age, sex, total intracranial volume, education years, and multiple sites from individual IC weights to minimize potential nuisance effects, before defining structural covariances (Fig. 1B).

Structural covariances of the A+W+ group were compared with those of the other 3 groups using Fisher's r-to-z transformation, where each correlation value was converted into normally distributed values. for example, Z_{A+W+} was calculated using the formula: 0.5 x [log(1+R_{A+W+}) – log(1-R_{A+W+})], and compared with $Z = (Z_{A+W+} - Z_{A-W-}) / \sqrt{[1/(N_{A+W+} -3) + 1/(N_{A-W-}-3)]}$, where N_{A+W+} and N_{A-W-} represent sample sizes for the A+W+ and A-W- groups, respectively. For ICs involved in structural covariances showing significant differences between groups, we further associated the weights with several patient group clinical scores (totals of A+W+, A+W-, and A-W+ groups), along with removing nuisance effects. Significant associations between each regional IC weight and amyloid PET SUVR, quantitative WMH volume, and clinical variables were investigated in all samples (Fig. 1B). Supplemental structural covariance analyses were also performed between regional gray matter volumes extracted by averaging the values at each cerebral region (a total of 90 regions) on the AAL atlas (Tzourio-Mazoyer et al., 2002).

All statistical analyses were performed using MATLAB (MathWorks, Sherborn, MA, USA) ("MATLAB - MathWorks - MATLAB & Simulink," n.d.)-based custom software. For inference on structural covariance, a false discovery rate (FDR) <0.1 and 0.15 thresholds were determined to be significant in addressing multiple comparison issues. FDR thresholding controls the expected proportion of false positives among structural covariances that exhibit significance (Genovese et al., 2002). FDR control levels in the range of 0.1–0.2 are known to be practically acceptable, as several neuroimaging studies have applied this criterion (Genovese et al., 2002; Gordon et al., 2018; Jung et al., 2019; Molteni et al., 2017; Yu et al., 2018).

3. Results

3.1. Group comparison of demographic, neuropsychological characteristics, and regional gray matter volume

The clinical characteristics of the patients in the 4 groups are compared in Tables 1 and 2. Briefly, the A+W+ group participants were older, more likely to be APOE ε4 allele carriers, and scored lower on several cognitive function tests compared to A-W- subjects.

3.2. Selected independent components as hypothesized structural covariance sources

Of the 59 stable ICs derived using the ICASSO procedure, we selected 13 ICs as hypothesized structural covariance sources, including 2 THL/BG networks (THL and BG), 3 CEN (superior parietal gyrus [SPG], middle frontal gyrus [MFG] 1 and 2), 3 SN (left insular [INS], insular/putamen [INS/PUT], dorsal anterior cingulate cortex [dACC]), 1 SMN (right supplementary motor area [SMA]), and 4 DMN (posterior cingulate cortex/precuneus[PCC/PRCU], hippocampus [HP], ventral anterior cingulate cortex [vACC], and right angular gyrus [ANG])-related regions (Supplementary Figure 1).

3.3. Associations of IC loadings among symptoms, amyloid PET SUVR and WMH volume

All significant associations between the IC weights and WMH volume and amyloid PET SUVR in the total sample are shown in Figs 2 A and B (FDR corrected $p < 0.1$). WMH volume increase was associated with an increase in IC weights of MGF and HP (i.e., positive correlation), while the IC weight of THL decreased when the WMH volume increased (i.e., negative correlation). On the other hand, the amyloid PET SUVR increase was positively correlated with the IC weights of the MFG and negatively correlated with the IC weight of HP.

In association studies on cognitive function tests and structural covariance network properties, all significant associations between the IC weights and clinical variables are detailed in Fig. 2 (C) (FDR corrected p <0.1). The CDR-SB score (the higher the score, the higher the severity of dementia) was correlated with the individual weights of the DMN [HP: negative, ANG: positive], SN [dACC: positive, INS: negative], CEN [MFG: positive, SPG: positive], and THL/BG network [THL: negative, BG: negative] areas, respectively. On the other hand, the cognitive function test scores, which indicated a good function as the score increased, showed opposite results to that of the CDR-SB.

3.4. Differences in structural covariances in the A+W+ group compared to A- or W- groups

Several structural covariances in the A+W+ group were significantly different from those in the A-W- group (Fig. 3 (A); FDR

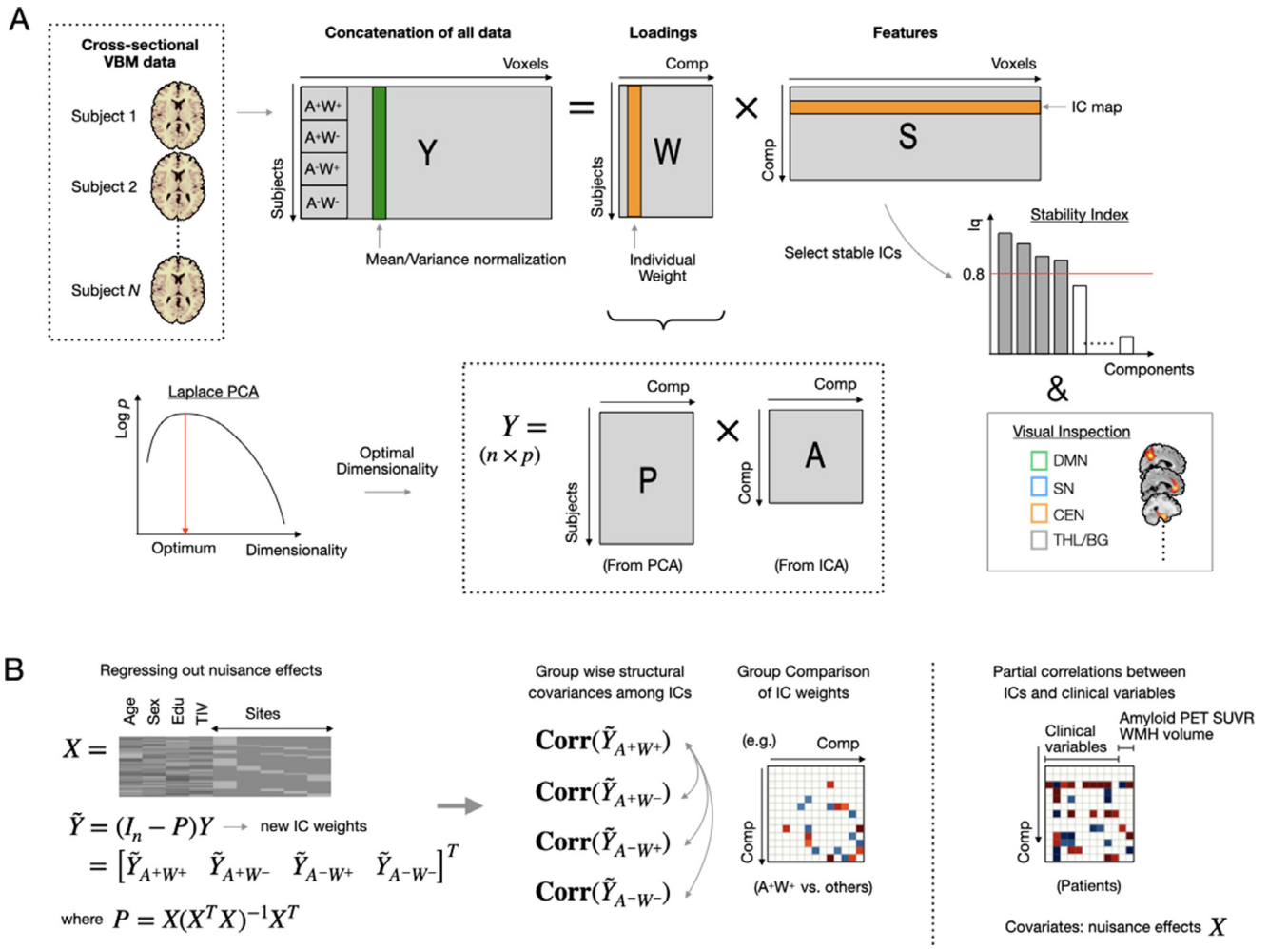

Fig. 1. Description of the structural covariance analysis process used in this study (A) Source-based morphometric analysis. (B) Structural covariance network analysis and group comparisons. Abbreviations: VBM, voxel-based morphometry; Comp, component; PCA, principal component analysis; ICA, independent component analysis; DMN, default mode network; SN, salience network; CEN, central executive network; THL, thalamus; BG, basal ganglia; Edu, education; TIV, total intracranial volume; IC, independent component; WMH, white matter hyperintensities; A+W+, amyloid deposition positive with moderate/severe WMH; A+W-, positive amyloid deposition without moderate/severe WMH; A-W+, negative amyloid deposition with moderate/severe WMH; A-W-, negative amyloid deposition without moderate/severe WMH.

corrected $p < 0.1$ or 0.15). A+W+ patients showed negative intranetwork structural association within the (i) DMN [between ANG and HP] and (ii) SN [between INS and dACC], and positive intranetwork structural association within the (iii) THL/BG. When examining the inter-network connectivity in A+W+ compared to A-W- groups, differences in associations between subnetwork regions could be observed as follows: (i) positive association: DMN and THL/BG [HP-THL, vACC-BG], DMN and SN [HP-INS, vACC-INS], DMN and CEN [ANG-MFG], DMN-SMN [PCC/PRCU-SMA], SN, and THL/BG [INS-THL/BG]; (ii) negative association: CEN and THL/BG [MFG-BG], CEN-SN [MFG-INS]. Other significant associations between the A+W+ and A+W-/A-W+ groups are shown in Fig. 3 (B), (C), and supplementary figure 2. The results of regional volume comparisons using VBM according to the group and correlation patterns of 90 regional gray matter volumes extracted from the AAL atlas for each group are also shown in supplementary table 4, supplementary figure 3, and supplementary figure 4.

4. Discussion

This study aimed to investigate whether amyloid deposition accompanied by CSVD was synergistically associated with altered anatomic connections of subcortico- and cortico-cortical networks in older adults with cognitive impairment. Our results revealed that SCN, in patients with both amyloid burden and CSVD, showed decreased intranetwork connectivity in the SN and DMN, increased cortico-subcortical internetwork connectivity in DMN and SN, decreased cortico-subcortical internetwork connectivity in CEN, and altered internetwork connectivity in DMN-SN-CEN. These findings suggest that the burdens of amyloid and CSVD individually or collectively can contribute to the wider disruption of anatomical organization of large-scale brain networks in cognitively impaired elderly individuals.

In the participants in our study, the volume of WMH was inversely associated with the structural covariance of MFG-THL and HP-THL (Fig. 2A). Nestor et al. reported that WMH volume is related to reduced fronto-subneocortical and PCC-subneocortical network characteristics in AD, suggesting that CSVD burden was an important etiological factor underlying the disruption of anatomic covariance networks (Nestor et al., 2017). Our results were generally concordant with this perspective of CSVD burden on network disruption, although it was not a connection with PCC but with HP that belonged to the same DMN. On the other hand, the reduced covarying regional volume between the HP and MFG networks was correlated with an increased amyloid PET SUVR (Fig. 2B). Brain MRI and PET studies conducted by La Joie et al. pro-

Table 1
Clinical characteristics of study participants according to amyloid deposition and WMH severity

	Amyloid negative		Amyloid positive		*p* value
	(A) WMH mild (N = 83) Mean (SD)/N (%)	(B) WMH moderate/severe (N = 81) Mean (SD)/N (%)	(C) WMH mild (N = 38) Mean (SD)/N (%)	(D) WMH moderate/severe (N = 41) Mean (SD)/N (%)	
Age (years)	69.87 (6.86)	73.33 (6.97)	69.87 (8.34)	77.24 (5.65)	< 0.001
Education (years)	7.42 (4.62)	6.93 (4.33)	9.70 (4.99)	8.45 (4.88)	0.015
Women (N, %)	56 (67.5)	59 (72.8)	27 (71.1)	26 (63.4)	0.724
APOE4 (N, %)					< 0.001
E4/E4	0 (0.0)	1 (1.2)	3 (7.9)	1 (2.4)	
E4/E3	8 (9.6)	14 (17.3)	19 (50.0)	19 (46.3)	
E4/E2	2 (2.4)	1 (1.2)	2 (5.3)	2 (4.9)	
E3/E3	58 (69.9)	56 (69.1)	13 (34.2)	18 (43.9)	
E3/E2	15 (18.1)	9 (11.1)	1 (2.6)	1 (2.4)	
E2/E2	0 (0.0)	0 (0.0)	0 (0.0)	0 (0.0)	
Comorbidity (N, %)					
Hypertension	36 (43.4)	53 (65.4)	15 (39.5)	29 (70.7)	0.001
Diabetes Mellitus	14 (16.9)	21 (25.9)	6 (15.8)	7 (17.1)	0.400
Hyperlipidemia	33 (39.8)	36 (44.4)	9 (23.7)	13 (31.7)	0.137
CVD	9 (10.8)	27 (33.3)	4 (10.5)	7 (17.1)	0.001
Lacunae (number)	0.26 (0.77)	2.57 (3.38)	0.26 (0.72)	1.45 (1.88)	< 0.001
WMH volume	1.09 (1.16)	8.97 (7.31)	0.88 (0.70)	9.76 (4.96)	< 0.001
Amyloid PET SUVR	0.58 (0.04)	0.60 (0.06)	0.87 (0.13)	0.88 (0.13)	< 0.001
CDR (N, %)					< 0.001
0	6 (7.2)	0 (0.0)	0 (0.0)	0 (0.0)	
0.5	69 (83.1)	63 (77.8)	19 (50.0)	28 (68.3)	
1	8 (9.6)	14 (17.3)	17 (44.7)	9 (22.0)	
2 or more	0 (0.0)	4 (5.1)	2 (5.3)	4 (9.7)	
CDR-Sum of Box (score)	1.86 (1.67)	2.77 (2.85)	4.11 (2.76)	3.73 (3.81)	< 0.001
Clinical Diagnosis (N, %)					< 0.001
SCD	19 (22.9)	10 (12.3)	0 (0.0)	4 (9.8)	
MCI	57 (68.7)	48 (59.3)	12 (31.6)	17 (41.5)	
AD	1 (1.2)	0 (0.0)	20 (52.6)	1 (2.4)	
AD with CSVD	0 (0.0)	2 (2.5)	0 (0.0)	16 (39.0)	
SVaD	0 (0.0)	19 (23.5)	0 (0.0)	3 (7.3)	

Analysis of variance or chi-square tests were conducted.
Abbreviations: WMH, white matter hyperintensities; SD, standard deviation; APOE, apolipoprotein E; CVD, cardiovascular disease; CDR, clinical dementia rating; SCD, subjective cognitive decline; MCI, mild cognitive impairment; AD, Alzheimer's disease; CSVD, small vessel disease; SVaD, subcortical vascular dementia; SUVR, standard uptake value ratio

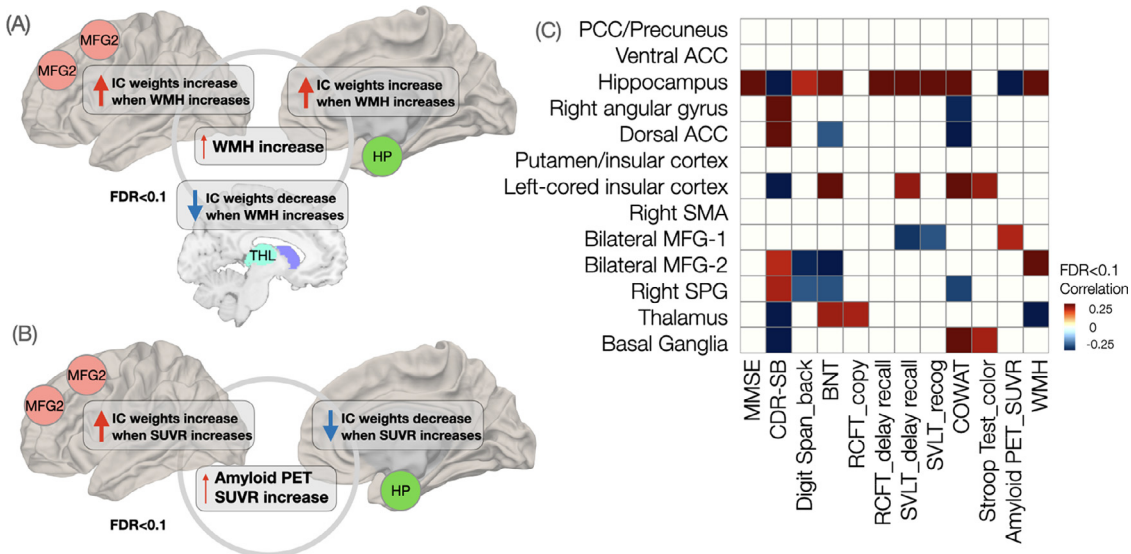

Fig. 2. Correlations between regional independent component weights and cognitive function test, amyloid PET SUVR or WMH volume All significant associations between the independent component (IC) weight and cognitive function/neuroimage measurement in the total sample are shown (FDR corrected $p < 0.1$). (A) Partial correlation between the IC weight and WMH volume. (B) Partial correlation between the IC weight and amyloid PET SUVR. (C) Partial correlation between IC weight and cognitive function test (z-score). All cognitive function test scores, except CDR-SB, indicated better cognitive function as they increased. The red arrow indicates that IC weights increase when the variables increase (i.e., positive correlation), while the blue arrow indicates that the IC weights decrease when the variables increase (i.e., negative correlation). The color of each region represents large-scale brain networks to which regions belong as follows: green-default mode network; pink-central executive network. Abbreviations: WMH, white matter hyperintensities; PET, positron emission tomography; SUVR, standardized uptake value ratio; CDR-SB, clinical dementia rating sum of box; Digit Span_back, digit span backward test; BNT, Boston naming test; RCFT, Rey complex figure test; SVLT, Seoul verbal learning test delayed recall; SVLT_recog, Seoul verbal learning test recognition; COWAT, controlled oral word association test; MFG, middle frontal gyrus; HP, hippocampus; THL, thalamus; PCC, posterior cingulate cortex; ACC, anterior cingulate cortex; SMA, supplementary motor area; false discovery rate, FDR (For interpretation of the references to color in this figure legend, the reader is referred to the Web version of this article.)

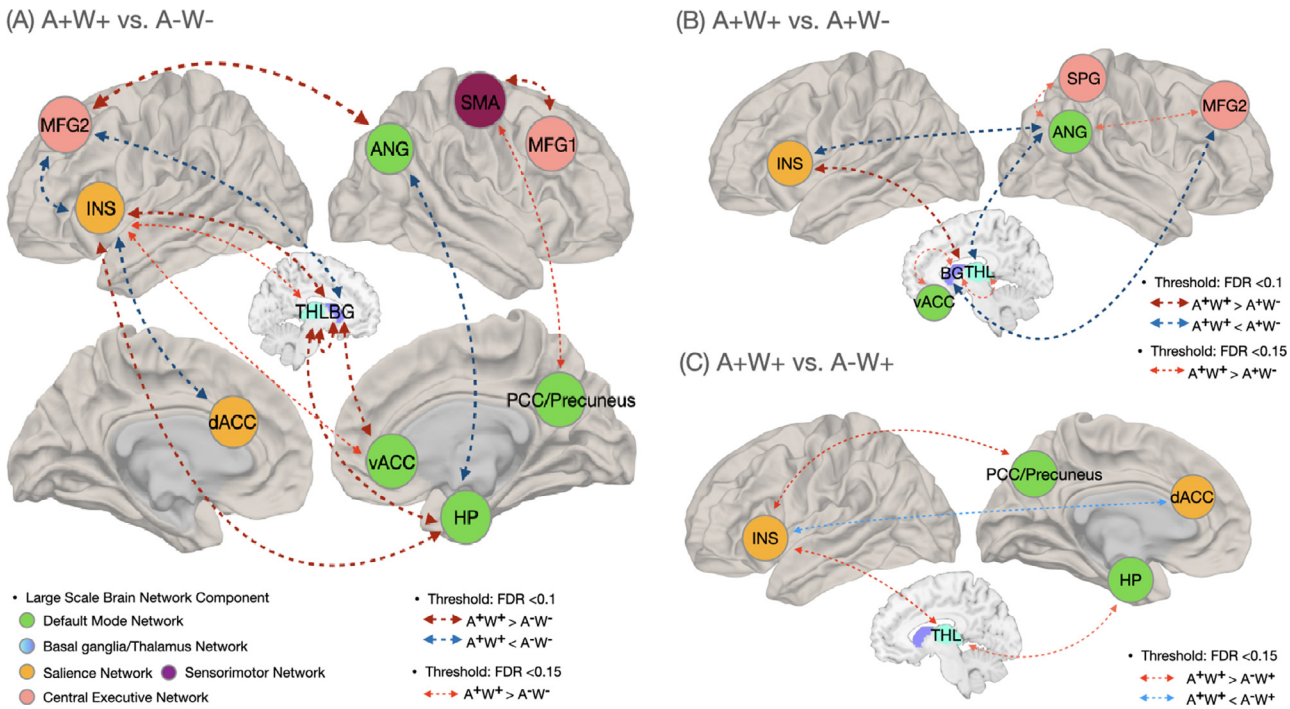

Fig. 3. Structural covariance network differences in the amyloid deposition with moderate/severe WMH group Structural covariances of the A+W+ group were compared with those of other groups (A-W-, A+W-, or A-W+) using Fisher's r-to-z transformation (FDR corrected $p < 0.1$ or 0.15). In the comparison of the A+W+ group with the other groups, the red line indicates increased connectivity, and the blue line indicates decreased connectivity in the A+W+ group. The color of each region represents large-scale brain networks to which the region belong. WMH, white matter hyperintensities; A+W+, amyloid deposition positive with moderate/severe WMH; A+W-, amyloid deposition-positive without moderate/severe WMH; A-W+, amyloid deposition negative with moderate/severe WMH; A-W-, amyloid deposition negative without moderate/severe WMH; MFG, middle frontal gyrus; INS, insular; ANG, angular gyrus; SMA, supplementary motor area; HP, hippocampus; PCC, posterior cingulate cortex; vACC, ventral anterior cingulate cortex; dACC, dorsal anterior cingulate cortex; THL, thalamus; BG, basal ganglia; FDR, false discovery rate (For interpretation of the references to color in this figure legend, the reader is referred to the Web version of this article.)

vided evidence for regional variations in the relationship between amyloid load and brain atrophy (La Joie et al., 2012). Our study also showed that amyloid burden was inversely related to the IC weight of HP and positively with that of MFG. Furthermore, this structural variance pattern was correlated with the CDR-SB and other cognitive test scores (Fig. 2C). A previous study by Li et al. showed that extensive SCN in the CEN in patients with positive Aβ status and dorsolateral prefrontal cortex-anchored peak cluster volumes correlated with cognitive performance, suggesting that the CEN plays a compensatory clinical role in the AD continuum (Li et al., 2019).

We investigated the combined effects of amyloid and WMH burden on SCN in terms of intra-and inter-network connectivity by comparing the A+W+ and A-W- groups. We demonstrated decreased structural covariance within not only the DMN (HP-ANG) but also within the SN (INS-dACC) in the A+W+ group, consistent with previous findings on functional intranetwork changes in AD (Brier et al., 2012). Conversely, an increase in SCN was observed within the BG-THL (Fig. 3A). Amyloid plaques were found to be preferentially deposited in regions of the DMN (Buckner et al., 2005), causing impaired resting-state fMRI connectivity (Selkoe et al., 2016). Similarly, in an SCN study, Montembeault et al. showed decreased structural association in the medial temporal lobe subsystem of the DMN, where the most prominent impact of the disease at early stages of AD presents (Montembeault et al., 2016). Brier et al. also reported that changes in SCN within the SN varied according to the severity of dementia in AD, with an increased correlation at CDR values between 0 and 0.5 and a reduced correlation at CDR values of 1 (Brier et al., 2012). We observed a loss of covarying regional volume within the SN even though 70% of our participants had CDR values less than 0.5. This could be an early characteristic change in the SCN when amyloid and CSVD burdens are both present.

In internetwork analyses of the A+W+ group compared to A-W-, we found increased cortico-subcortical structural covariances in the DMN (vACC-BG, HP-THL) and SN (INS-THL/BG), and decreased cortico-subcortical structural covariances in the CEN (MFG-BG). A previous study provided a functional connectivity map of the subcortical-DMN in the human brain (Li et al., 2021). In particular, HP and THL show functional connectivity, presumably representing synchronous changes in blood flow and are closely related to memory (Aggleton et al., 2010; Baumgartner et al., 2018; Stein et al., 2000). The connection between THL and INS is also known to be related to salient information and emotional processing (Ghaziri et al., 2018). In this study, we observed brain atrophy in conjunction with increased structural covariance in these structurally connected areas, in A+W+ group compared to the A-W- group (Supplementary Table 2). On the other hand, we observed a decreased structural covariance between subcortical and CEN areas in the A+W+ group. These patterns were prominent in comparison with non-WMH groups, irrespective of amyloid deposition (Fig. 3 A and B), suggesting that it was related to vascular factors.

In addition, we observed altered cortico-cortical SCN in the DMN-SN-CEN in the A+W+ group. Our results indicated that the SCN of the A+W+ group was characterized by (a) increased structural covariance of DMN-SN (HP-INS) and DMN-CEN (ANG-MFG) and (b) decreased structural covariance of CEN-SN (MFG-INS). Convergent evidence has suggested that the DMN, SN, and CEN show interactive and dynamic changes with neuropathological progression (Agosta et al., 2012; Myers et al., 2014; Uddin, 2015; Wang et al., 2015). Our findings are consistent with previous studies showing decreased DMN integrity (Andrews-Hanna et al., 2007;

Table 2
Neuropsychological test scores of study participants according to amyloid deposition and WMH severity

	Amyloid negative (A)	(B)	Amyloid positive (C)	(D)	*p* value	Post hoc
	WMH mild (N = 83) Mean (SD)	WMH moderate/severe (N = 81) Mean (SD)	WMH mild (N = 38) Mean (SD)	WMH moderate/severe (N = 41) Mean (SD)		
MMSE (score)	25.12 (3.60)	23.16 (5.23)	20.82 (5.65)	21.62 (5.38)	< 0.001	A>C, A>D
Neurocognitive Test (Z score)						
Digit span-backward	-0.17 (1.08)	-0.55 (1.01)	-0.76 (1.28)	-0.82 (0.98)	0.004	A>C, A>D
Boston Naming Test	-0.25 (1.13)	-0.92 (1.45)	-0.87 (2.07)	-1.38 (1.90)	0.01	A>D
RCFT-copy	-0.68 (1.35)	-0.44 (4.77)	-2.01 (3.30)	-1.70 (2.63)	0.04	n.s.
RCFT-delayed recall	-0.45 (1.22)	-0.93 (1.08)	-1.73 (1.20)	-1.40 (1.23)	< 0.001	A>C, A>D, B>C
SVLT-delayed recall	-0.51 (1.15)	-0.87 (1.20)	-1.79 (1.81)	-1.52 (1.65)	< 0.001	A>C, A>D, B>C
SVLT-recognition	-0.28 (1.07)	-0.68 (0.96)	-1.52 (1.00)	-1.01 (1.15)	< 0.001	A>C, A>D, B>C
COWAT animal	-0.22 (1.02)	-0.87 (1.19)	-1.17 (1.11)	-1.13 (1.26)	< 0.001	A>C, A>B, A>D
Stroop Test-color	-0.40 (1.27)	-0.99 (1.34)	-1.59 (1.82)	-1.01 (1.58)	< 0.001	A>C

Analysis of variance and Bonferroni correction for multiple comparisons were conducted.
Abbreviations: WMH, white matter hyperintensities; SD, standard deviation; MMSE, mini mental status examination; SGDS, short-form geriatric depression scale; RCFT, Rey Complex figure Test; SVLT, Seoul Verbal Learning Test; COWAT, Controlled Oral Word Association Test.

Chen et al., 2011; Siman-Tov et al., 2017) and increased structural association in the DMN and SN as compensatory inter-network changes (Aboud et al., 2019; Hohenfeld et al., 2018; Li et al., 2019). It has been suggested that increased CEN functional connectivity may be a compensatory mechanism to cope with CSVD burden (Chong et al., 2019) leading to aberrations in these networks. In the A+W+ group, increased SCN of DMN-SN was seen when compared with A- groups (Fig. 3 A and C) and increased SCN of DMN-CEN was seen when compared with W- groups (Fig. 3 A and B), suggesting that these changes may be associated with amyloid and CSVD burdens alone, respectively. These characteristics and decreased SCN of CEN-SN in the A+W+ group also had a significant association with cognitive function measures, such as the CDR-SB score (Fig. 2 B). Given that our subjects were at a relatively mild stage of cognitive impairment, our results suggest a despecialization of brain areas resulting in compensatory inter-network "cross-talk" to support regions with deteriorating functions (Montembeault et al., 2016; Zhou et al., 2010). Moreover, these patterns of SCN in the A+W+ group might indicate that amyloid deposition and CSVD seem to be associated with individually and collectively altered brain structural networks and need to be considered when assessing network disruption in case of co-morbidities.

Some limitations of our study are discussed here. First, our cross-sectional design did not allow us to make causal inferences regarding the relationship between amyloid burden and WMH. Second, MRI data were collected using various scanner types and imaging protocols. We analyzed the differences in SCN among the groups after adjusting for data gathering sites, but this remains a potential source of heterogeneity. Third, although we excluded other types of dementia based on clinical diagnosis criteria, cerebrospinal fluid or neuroimaging biomarkers except amyloid deposition and neurodegeneration could not be considered as factors for identifying SCN changes related to amyloid or CSVD abnormalities in the brain. In particular, tau pathology is known to be closely associated with clinical symptoms, and lack of assessment of tau is an important limitation for addressing the National Institute on Aging and Alzheimer's Association AT(N) research framework in this study (Jack Jr. et al., 2018). In addition, the A-W- group was used as a de facto control group but different from a cognitively healthy group. Lastly, even though we have presented our main findings with FDR <0.1 and 0.15 thresholds as practically acceptable, further studies with larger datasets are required to improve the level of statistical significance. Future studies examining the effects of both tau and Aβ on SCN may further enhance our understanding of the vulnerable characteristics of structural integrity of the brain structural network in older adults with cognitive impairment.

5. Conclusions

Our study used the SBM method to demonstrate SCN characteristics related to amyloid burden occurring in conjunction with CSVD, represented by decreased intranetwork connectivity and increased cortico-cortical or cortico-subcortical internetwork connectivity in the SN and DMN regions, and decreased cortico-cortical and cortico-subcortical internetwork connectivity in the CEN. This is a unique study investigating SCN-based ICA networks, and our results support the notion that amyloid deposition and CSVD represented by WMH are associated with individually and collectively altered brain networks. We also suggest that the study of structural covariances is valuable to better understand network-level anatomical changes in the presence of neurodegenerative and cerebrovascular factors. Nevertheless, further research on this subject is required.

Availability of data and material

The datasets analyzed during the current study are available from the first and corresponding authors on reasonable request.

Authors contribution

Sang Joon Son: acquisition of clinical data, manuscript preparation, study conception, and design. Chang Hyung Hong: Acquisition of clinical data. Na-Rae Kim: imaging, statistical analysis, manuscript preparation. Jin Wook Choi: Imaging and statistical analysis. Hyun Woong Roh: Study coordination. Heirim Lee: Imaging and statistical analysis. Sang Won Seo: Acquisition of clinical data. Seong Hye Choi: Acquisition of clinical data. Eun-Joo Kim: acquisition of clinical data. Byeong C. Kim: acquisition of clinical data. Seong Yoon Kim: Acquisition of clinical data. Jaeyoun Cheong: study coordination. So Young Moon: Acquisition of clinical data Bumhee Park: imaging and statistical analysis, manuscript preparation, study conception, and design.

Disclosure statement

The authors have no actual or potential conflicts of interest.

This study was conducted with biospecimens and data from the biobank of the Chronic Cerebrovascular Disease Consortium. The consortium was supported and funded by the Korea Centers for Disease Control and Prevention (# 4845-303). This work was also supported by the National Research Foundation of Korea (NRF) funded by the Ministry of Science and ICT (NRF-2019R1A5A2026045).

Acknowledgements

We thank the staff of the Suwon Geriatric Mental Health Center for their involvement in data acquisition.

Supplementary materials

Supplementary material associated with this article can be found, in the online version, at doi:10.1016/j.neurobiolaging.2022.05.010.

References

Aboud, K.S., Huo, Y., Kang, H., Ealey, A., Resnick, S.M., Landman, B.A., Cutting, L.E., 2019. Structural covariance across the lifespan: Brain development and aging through the lens of inter-network relationships. Hum. Brain Mapp 40, 125–136. doi:10.1002/hbm.24359.

Aggleton, J.P., O'Mara, S.M., Vann, S.D., Wright, N.F., Tsanov, M., Erichsen, J.T., 2010. Hippocampal-anterior thalamic pathways for memory: Uncovering a network of direct and indirect actions. Eur. J. Neurosci. 31, 2292–2307. doi:10.1111/j.1460-9568.2010.07251.x.

Agosta, F., Pievani, M., Geroldi, C., Copetti, M., Frisoni, G.B., Filippi, M., 2012. Resting state fMRI in Alzheimer's disease: beyond the default mode network. Neurobiol. Aging 33, 1564–1578. doi:10.1016/j.neurobiolaging.2011.06.007.

Ahn, H.J., Chin, J., Park, A., Lee, B.H., Suh, M.K., Seo, S.W., Na, D.L., 2010. Seoul neuropsychological screening battery-dementia version (SNSB-D): A useful tool for assessing and monitoring cognitive impairments in dementia patients. J. Korean Med. Sci. 25, 1071–1076. doi:10.3346/jkms.2010.25.7.1071.

Alexander-Bloch, A., Giedd, J.N., Bullmore, E., 2013a. Imaging structural co-variance between human brain regions. Nat. Rev. Neurosci. 14, 322–336. doi:10.1038/nrn3465.

Alexander-Bloch, A., Raznahan, A., Bullmore, E., Giedd, J., 2013b. The convergence of maturational change and structural covariance in human cortical networks. J. Neurosci. 33, 2889–2899. doi:10.1523/JNEUROSCI.3554-12.2013.

American Psychiatric Association, 2013. Diagnostic and Statistical Manual of Mental Disorders, 5th ed. American Psychiatric Association Publishing doi:10.1176/appi.books.9780890425596.

Andrews-Hanna, J.R., Snyder, A.Z., Vincent, J.L., Lustig, C., Head, D., Raichle, M.E.E., Buckner, R.L., 2007. Disruption of large-scale brain systems in advanced aging. Neuron 56, 924–935. doi:10.1016/j.neuron.2007.10.038.

Ashburner, J., 2007. A fast diffeomorphic image registration algorithm. Neuroimage 38, 95–113. doi:10.1016/j.neuroimage.2007.07.007.

Ashburner, J., Friston, K.J., 2000. Voxel-based morphometry - the methods. Neuroimage 11, 805–821. doi:10.1006/nimg.2000.0582.

Baumgartner, P., El Amki, M., Bracko, O., Luft, A.R., Wegener, S., 2018. Sensorimotor stroke alters hippocampo-thalamic network activity. Sci. Rep. 8, 1–11. doi:10.1038/s41598-018-34002-9.

Beckmann, C.F., Smith, S.M., 2004. Probabilistic independent component analysis for functional magnetic resonance imaging. IEEE Trans. Med. Imaging 23, 137–152. doi:10.1109/TMI.2003.822821.

Brenowitz, W.D., Hubbard, R.A., Keene, C.D., Hawes, S.E., Longstreth, W.T.T., Woltjer, R.L., Kukull, W.A., 2017. Mixed neuropathologies and estimated rates of clinical progression in a large autopsy sample. Alzheimer's dement. 13, 654–662. doi:10.1016/j.jalz.2016.09.015

Brier, M.R., Thomas, J.B., Snyder, A.Z., Benzinger, T.L., Zhang, D., Raichle, M.E., Holtzman, D.M., Morris, J.C., Ances Dr, B.M., 2012. Loss of intranetwork and internetwork resting state functional connections with Alzheimer's disease progression. J. Neurosci. 32, 8890–8899. doi:10.1523/JNEUROSCI.5698-11.2012.

Bucci, M., Savitcheva, I., Farrar, G., Salvadó, G., Collij, L., Doré, V., Gispert, J.D., Gunn, R., Hanseeuw, B., Hansson, O., Shekari, M., Lhommel, R., Molinuevo, J.L., Rowe, C., Sur, C., Whittington, A., Buckley, C., Nordberg, A., 2021. A multisite analysis of the concordance between visual image interpretation and quantitative analysis of [18F]flutemetamol amyloid PET images. Eur. J. Nucl. Med. Mol. Imaging 48, 2183–2199. doi:10.1007/s00259-021-05311-5.

Buckner, R.L., Snyder, A.Z., Shannon, B.J., LaRossa, G., Sachs, R., Fotenos, A.F., Sheline, Y.I., Klunk, W.E., Mathis, C.A., Morris, J.C., Mintun, M.A., 2005. Molecular, structural, and functional characterization of Alzheimer's disease: evidence for a relationship between default activity, amyloid, and memory. J Neurosci 25, 7709–7717 25/34/7709[pii]10.1523/JNEUROSCI.2177-05.2005.

Cacciaglia, R., Molinuevo, J.L., Falcón, C., Arenaza-Urquijo, E.M., Sánchez-Benavides, G., Brugulat-Serrat, A., Blennow, K., Zetterberg, H., Gispert, J.D., 2020. APOE-ε4 shapes the cerebral organization in cognitively intact individuals as reflected by structural gray matter networks. Cereb. Cortex 30, 4110–4120. doi:10.1093/cercor/bhaa034.

Chen, Z.J., He, Y., Rosa-Neto, P., Gong, G., Evans, A.C., 2011. Age-related alterations in the modular organization of structural cortical network by using cortical thickness from MRI. Neuroimage 56, 235–245. doi:10.1016/j.neuroimage.2011.01.010.

Chong, J.S.X., Jang, H., Kim, H.J., Ng, K.K., Na, D.L., Lee, J.H., Seo, S.W., Zhou, J., 2019. Amyloid and cerebrovascular burden divergently influence brain functional network changes over time. Neurology 93, e1514–e1525. doi:10.1212/WNL.0000000000008315.

Chui, H.C., Zarow, C., Mack, W.J., Ellis, W.G., Jagust, W.J., Mungas, D., Reed, B.R., Kramer, J.H., DeCarli, C.C., Weiner, M.W., Vinters, H.V, 2006. Cognitive impact of subcortical vascular and alzheimer's disease pathology. Ann. Neurol. 60, 677–687.

Doody, R.S., Thomas, R.G., Farlow, M., Iwatsubo, T., Vellas, B., Joffe, S., Kieburtz, K., Raman, R., Sun, X., Aisen, P.S., Siemers, E., Liu-Seifert, H., Mohs, R., 2014. Phase 3 trials of solanezumab for mild-to-moderate alzheimer's disease. N. Engl. J. Med. doi:10.1056/NEJMoa1312889.

Duan, K., Premi, E., Pilotto, A., Cristillo, V., Benussi, A., Libri, I., Giunta, M., Bockholt, H.J., Liu, J., Campora, R., Pezzini, A., Gasparotti, R., Magoni, M., Padovani, A., Calhoun, V.D., 2021. Alterations of frontal-temporal gray matter volume associate with clinical measures of older adults with COVID-19. Neurobiol. Stress 14, 100326. doi:10.1016/j.ynstr.2021.100326.

Evans, A.C., 2013. Networks of anatomical covariance. Neuroimage 80, 489–504. doi:10.1016/j.neuroimage.2013.05.054.

Fazekas, F., Chawluk, J.B., Alavi, A., Hurtig, H.I., Zimmerman, R.A., 1987. MR signal abnormalities at 1.5 T in Alzheimer's dementia and normal aging. Am. J. Roentgenol. 149, 351–356. doi:10.2214/ajr.149.2.351.

Foster-Dingley, J.C., Hafkemeijer, A., Van Den Berg-Huysmans, A.A., Moonen, J.E.F., De Ruijter, W., De Craen, A.J.M., Van Der Mast, R.C., Rombouts, S.A.R.B., Van Der Grond, J., 2016. Structural covariance networks and their association with age, features of cerebral small-vessel disease, and cognitive functioning in older persons. Brain Connect 6, 681–690. doi:10.1089/brain.2016.0434.

Genovese, C.R., Lazar, N.A., Nichols, T., 2002. Thresholding of statistical maps in functional neuroimaging using the false discovery rate. Neuroimage 15, 870–878. doi:10.1006/nimg.2001.1037.

Ghaziri, J., Tucholka, A., Girard, G., Boucher, O., Houde, J.C., Descoteaux, M., Obaid, S., Gilbert, G., Rouleau, I., Nguyen, D.K., 2018. Subcortical structural connectivity of insular subregions. Sci. Rep. 8, 1–12. doi:10.1038/s41598-018-26995-0.

Gordon, B.A., McCullough, A., Mishra, S., Blazey, T.M., Su, Y., Christensen, J., Dincer, A., Jackson, K., Hornbeck, R.C., Morris, J.C., Ances, B.M., Benzinger, T.L.S., 2018. Cross-sectional and longitudinal atrophy is preferentially associated with tau rather than amyloid β positron emission tomography pathology. Alzheimer's Dement. Diagnosis. Assess. Dis. Monit. doi:10.1016/j.dadm.2018.02.003.

Hardy, J., De Strooper, B., 2017. Alzheimer's disease: Where next for anti-amyloid therapies? Brain 140, 853–855. doi:10.1093/brain/awx059.

Himberg, J., Hyvärinen, A., Esposito, F., 2004. Validating the independent components of neuroimaging time series via clustering and visualization. Neuroimage 22, 1214–1222. doi:10.1016/j.neuroimage.2004.03.027.

Hoagey, D.A., Rieck, J.R., Rodrigue, K.M., Kennedy, K.M., 2019. Joint contributions of cortical morphometry and white matter microstructure in healthy brain aging: A partial least squares correlation analysis. Hum. Brain Mapp 40, 5315–5329. doi:10.1002/hbm.24774.

Hohenfeld, C., Werner, C.J., Reetz, K., 2018. Resting-state connectivity in neurodegenerative disorders: Is there potential for an imaging biomarker? NeuroImage Clin doi:10.1016/j.nicl.2018.03.013.

Hwang, J., Jeong, J.H., Yoon, S.J., Park, K.W., Kim, E.-J.J., Yoon, B., Jang, J.-W.W., Kim, H.J., Hong, J.Y., Lee, J.-M.M., Park, H., Kang, J.-H.H., Choi, Y.-H.H., Park, G., Hong, J.Y., Byun, M.S., Yi, D., Kim, Y.K., Lee, D.Y., Choi, S.H., 2019. Clinical and biomarker characteristics according to clinical spectrum of Alzheimer's Disease (AD) in the validation cohort of Korean brain aging study for the early diagnosis and prediction of AD. J. Clin. Med. 8, 341. doi:10.3390/jcm8030341.

Hyvärinen, A., 1999. Fast and robust fixed-point algorithms for independent component analysis. IEEE Trans. Neural Networks. doi:10.1109/72.761722.

Jack Jr., C.R., Bennett, D.A., Blennow, K., Carrillo, M.C., Dunn, B., Haeberlein, S.B., Holtzman, D.M., Jagust, W., Jessen, F., Karlawish, J., Liu, E., Molinuevo, J.L., Montine, T., Phelps, C., Rankin, K.P., Rowe, C.C., Scheltens, P., Siemers, E., Snyder, H.M., Sperling, R., 2018. NIA-AA research framework: toward a biological definition of Alzheimer's disease. Alzheimers Dement 14, 535–562. doi:10.1016/j.jalz.2018.02.018.

Jung, K.I., Park, M.H., Park, B., Kim, S.Y., Kim, Y.O., Kim, B.N., Park, S., Song, C.H., 2019. Cerebellar gray matter volume, executive function, and insomnia: gender differences in adolescents. Sci. Rep. doi:10.1038/s41598-018-37154-w.

Kakeda, S., Watanabe, K., Nguyen, H., Katsuki, A., Sugimoto, K., Igata, N., Abe, O., Yoshimura, R., Korogi, Y., 2020. An independent component analysis reveals brain structural networks related to TNF-α in drug-naïve, first-episode major depressive disorder: a source-based morphometric study. Transl. Psychiatry 10, 187. doi:10.1038/s41398-020-00873-8.

Kang, Y, N.D.L., 2003. Seoul Neuropsychological Screening Battery (SNSB). Seoul Hum. Brain Res. Consult. Co.

Kapasi, A., DeCarli, C., Schneider, J.A., 2017. Impact of multiple pathologies on the threshold for clinically overt dementia. Acta Neuropathol 134, 171–186. doi:10.1007/s00401-017-1717-7.

La Joie, R., Perrotin, A., Barré, L., Hommet, C., Mézenge, F., Ibazizene, M., Camus, V., Abbas, A., Landeau, B., Guilloteau, D., de La Sayette, V., Eustache, F., Desgranges, B., Chételat, G., 2012. Region-specific hierarchy between atrophy, hypometabolism, and 2-amyloid (Aβ) load in Alzheimer's disease dementia. J. Neurosci. 32, 16265–16273. doi:10.1523/JNEUROSCI.2170-12.2012.

Li, J., Curley, W.H., Guerin, B., Dougherty, D.D., Dalca, A.V., Fischl, B., Horn, A., Edlow, B.L., 2021. Mapping the subcortical connectivity of the human default mode network. bioRxiv 2021.07.13.452265. Neuroimage 245, 118758. doi: 10.1016/j.neuroimage.2021.118758.

Li, K., Luo, X., Zeng, Q., Huang, P., Shen, Z., Xu, X., Xu, J., Wang, C., Zhou, J., Zhang, M., 2019. Gray matter structural covariance networks changes along the Alzheimer's disease continuum. NeuroImage Clin 23, 101828. doi:10.1016/j.nicl.2019.101828.

McKhann, G.M., Knopman, D.S., Chertkow, H., Hyman, B.T., Jack, C.R., Kawas, C.H., Klunk, W.E., Koroshetz, W.J., Manly, J.J., Mayeux, R., Mohs, R.C., Morris, J.C., Rossor, M.N., Scheltens, P., Carrillo, M.C., Thies, B., Weintraub, S., Phelps, C.H., 2011. The diagnosis of dementia due to Alzheimer's disease: recommendations from the national institute on aging-Alzheimer's association workgroups on diagnostic guidelines for Alzheimer's disease. Alzheimer's dement. 7, 263–269. doi:10.1016/j.jalz.2011.03.005

Mechelli, A., 2005. Structural covariance in the human cortex. J. Neurosci. 25, 8303–8310. doi:10.1523/JNEUROSCI.0357-05.2005.

Molteni, E., Rocca, M.A., Strazzer, S., Pagani, E., Colombo, K., Arrigoni, F., Boffa, G., Copetti, M., Pastore, V., Filippi, M., 2017. A diffusion tensor magnetic resonance imaging study of pediatric patients with severe non-traumatic brain injury. Dev. Med. Child Neurol. doi:10.1111/dmcn.13332.

Montembeault, M., Rouleau, I., Provost, J.S., Brambati, S.M., 2016. Altered gray matter structural covariance networks in early stages of Alzheimer's disease. Cereb. Cortex 26, 2650–2662. doi:10.1093/cercor/bhv105.

Morris, J.C., 1993. The Clinical Dementia Rating (CDR): current version and scoring rules. Neurology 43, 2412–2414. doi:10.1212/wnl.43.11.2412-a.

Murley, A.G., Coyle-Gilchrist, I., Rouse, M.A., Jones, P.S., Li, W., Wiggins, J., Lansdall, C., Rodríguez, P.V., Wilcox, A., Tsvetanov, K.A., Patterson, K., Lambon Ralph, M.A., Rowe, J.B., 2020. Redefining the multidimensional clinical phenotypes of frontotemporal lobar degeneration syndromes. Brain 143, 1555–1571. doi:10.1093/brain/awaa097.

Myers, N., Pasquini, L., Göttler, J., Grimmer, T., Koch, K., Ortner, M., Neitzel, J., Mühlau, M., Förster, S., Kurz, A., Förstl, H., Zimmer, C., Wohlschläger, A.M., Riedl, V., Drzezga, A., Sorg, C., 2014. Within-patient correspondence of amyloid-β and intrinsic network connectivity in Alzheimer's disease. Brain 137, 2052–2064. doi:10.1093/brain/awu103.

Nestor, S.M., Mišić, B., Ramirez, J., Zhao, J., Graham, S.J., Verhoeff, N.P.L.G., Stuss, D.T., Masellis, M., Black, S.E., 2017. Small vessel disease is linked to disrupted structural network covariance in Alzheimer's disease. Alzheimer's Dement. 13, 749–760. doi:10.1016/j.jalz.2016.12.007.

Noh, Y., Lee, Y., Seo, S.W., Jeong, J.H., Choi, S.H., Back, J.H., Woo, S.Y., Kim, G.H., Shin, J.S., Kim, C.H., Cho, H., Park, J.S., Lee, J.M., Hong, C.H., Kim, Sang Yun, Lee, J.H., Kim, Seong Yoon, Park, K.H., Han, S.H., Cheong, H.K., Na, D.L., 2014. A new classification system for ischemia using a combination of deep and periventricular white matter hyperintensities. J. Stroke Cerebrovasc. Dis. 23, 636–642. doi:10.1016/j.jstrokecerebrovasdis.2013.06.002.

Richmond, S., Johnson, K.A., Seal, M.L., Allen, N.B., Whittle, S., 2016. Development of brain networks and relevance of environmental and genetic factors: A systematic review. Neurosci. Biobehav. Rev. 71, 215–239. doi:10.1016/j.neubiorev.2016.08.024.

Roh, H.W., Choi, J., Kim, N., Kim, Y.S., Choi, J.W., Cho, S., Seo, S.W., Park, B., Hong, C.H., Yoon, D., Son, S.J., Kim, E.Y., 2020. Associations of rest-activity patterns with amyloid burden, medial temporal lobe atrophy, and cognitive impairment. EBioMedicine 58, 102881. doi:10.1016/j.ebiom.2020.102881.

Ryu, W.S., Woo, S.H., Schellingerhout, D., Chung, M.K., Kim, C.K., Jang, M.U., Park, K.J., Hong, K.S., Jeong, S.W., Na, J.Y., Cho, K.H., Kim, J.T., Kim, B.J., Han, M.K., Lee, Jun, Cha, J.K., Kim, D.H., Lee, S.J., Ko, Y., Cho, Y.J., Lee, B.C., Yu, K.H., Oh, M.S., Park, J.M., Kang, K., Lee, K.B., Park, T.H., Lee, Juneyoung, Choi, H.K., Lee, K., Bae, H.J., Kim, D.E., 2014. Grading and interpretation of white matter hyperintensities using statistical maps. Stroke 45, 3567–3575. doi:10.1161/STROKEAHA.114.006662.

Scheltens, P., Barkhof, F., Leys, D., Pruvo, J.P., Nauta, J.J.P., Vermersch, P., Steinling, M., Valk, J., 1993. A semiquantative rating scale for the assessment of signal hyperintensities on magnetic resonance imaging. J. Neurol. Sci. 114, 7–12. doi:10.1016/0022-510X(93)90041-V.

Schneider, L., 2020. A resurrection of aducanumab for Alzheimer's disease. Lancet Neurol 19, 111–112. doi:10.1016/S1474-4422(19)30480-6.

Seeley, W.W., Crawford, R.K., Zhou, J., Miller, B.L., Greicius, M.D., 2009. Neurodegenerative diseases target large-scale human brain networks. Neuron 62, 42–52. doi:10.1016/j.neuron.2009.03.024.

Seidlitz, J., Váša, F., Shinn, M., Romero-Garcia, R., Whitaker, K.J., Vértes, P.E., Wagstyl, K., Kirkpatrick Reardon, P., Clasen, L., Liu, S., Messinger, A., Leopold, D.A., Fonagy, P., Dolan, R.J., Jones, P.B., Goodyer, I.M., Raznahan, A., Bullmore, E.T., 2018. Morphometric similarity networks detect microscale cortical organization and predict inter-individual cognitive variation. Neuron 97, 231–247. doi:10.1016/j.neuron.2017.11.039, e7.

Selkoe, D.J., Hardy, J., Selkoe, D.J., Hardy, J., 2016. The amyloid hypothesis of Alzheimer's disease at 25 years. EMBO Mol Med 8, 595–608.

Siman-Tov, T., Bosak, N., Sprecher, E., Paz, R., Eran, A., Aharon-Peretz, J., Kahn, I., 2017. Early age-related functional connectivity decline in high-order cognitive networks. Front. Aging Neurosci. 8. doi:10.3389/fnagi.2016.00330.

Soriano-Mas, C., Harrison, B.J., Pujol, J., López-Solà, M., Hernández-Ribas, R., Alonso, P., Contreras-Rodríguez, O., Giménez, M., Blanco-Hinojo, L., Ortiz, H., Deus, J., Menchón, J.M., Cardoner, N., 2013. Structural covariance of the neostriatum with regional gray matter volumes. Brain Struct. Funct. 218, 697–709. doi:10.1007/s00429-012-0422-5.

Spreng, R.N., DuPre, E., Ji, J.L., Yang, G., Diehl, C., Murray, J.D., Pearlson, G.D., Anticevic, A., 2019. Structural covariance reveals alterations in control and salience network integrity in chronic schizophrenia. Cereb. Cortex 29, 5269–5284. doi:10.1093/cercor/bhz064.

Stein, T., Moritz, C., Quigley, M., Cordes, D., Haughton, V., Meyerand, E., 2000. Functional connectivity in the thalamus and hippocampus studied with functional MR imaging. Am. J. Neuroradiol. 21, 1397–1401.

Tzourio-Mazoyer, N., Landeau, B., Papathanassiou, D., Crivello, F., Etard, O., Delcroix, N., Mazoyer, B., Joliot, M., 2002. Automated anatomical labeling of activations in SPM using a macroscopic anatomical parcellation of the MNI MRI single-subject brain. Neuroimage 15, 273–289. doi:10.1006/nimg.2001.0978.

Uddin, L.Q., 2015. Salience processing and insular cortical function and dysfunction. Nat. Rev. Neurosci. 16, 55–61. doi:10.1038/nrn3857.

Wang, P., Zhou, B., Yao, H., Zhan, Y., Zhang, Z., Cui, Y., Xu, K., Ma, J., Wang, L., An, N., Zhang, X., Liu, Y., Jiang, T., 2015. Aberrant intra-and inter-network connectivity architectures in Alzheimer's disease and mild cognitive impairment. Sci. Rep. 5, 1–12. doi:10.1038/srep14824.

Winblad, B., Amouyel, P., Andrieu, S., Ballard, C., Brayne, C., Brodaty, H., Cedazo-Minguez, A., Dubois, B., Edvardsson, D., Feldman, H., Fratiglioni, L., Frisoni, G.B., Gauthier, S., Georges, J., Graff, C., Iqbal, K., Jessen, F., Johansson, G., Jönsson, L., Kivipelto, M., Knapp, M., Mangialasche, F., Melis, R., Nordberg, A., Rikkert, M.O., Qiu, C., Sakmar, T.P., Scheltens, P., Schneider, L.S., Sperling, R., Tjernberg, L.O., Waldemar, G., Wimo, A., Zetterberg, H., 2016. Defeating Alzheimer's disease and other dementias: a priority for European science and society. Lancet. Neurol. 15, 455–532. doi:10.1016/S1474-4422(16)00062-4.

Winblad, B., Palmer, K., Kivipelto, M., Jelic, V., Fratiglioni, L., Wahlund, L.O., Nordberg, A., Bäckman, L., Albert, M., Almkvist, O., Arai, H., Basun, H., Blennow, K., De Leon, M., Decarli, C., Erkinjuntti, T., Giacobini, E., Graff, C., Hardy, J., Jack, C., Jorm, A., Ritchie, K., Van Duijn, C., Visser, P., Petersen, R.C., 2004. Mild cognitive impairment - Beyond controversies, towards a consensus: report of the international working group on mild cognitive impairment, in: journal of internal medicine. J Intern Med 240–246. doi:10.1111/j.1365-2796.2004.01380.x.

Xu, L., Groth, K.M., Pearlson, G., Schretlen, D.J., Calhoun, V.D., 2009. Source-based morphometry: the use of independent component analysis to identify gray matter differences with application to schizophrenia. Hum. Brain Mapp. 30, 711–724. doi:10.1002/hbm.20540.

Ye, B.S., Seo, S.W., Kim, J.-H., Kim, G.H., Cho, H., Noh, Y., Kim, H.J., Yoon, C.W., Woo, S., Kim, S.H., Park, H.K., Kim, S.T., Choe, Y.S., Lee, K.H., Kim, J.S., Oh, S.J., Kim, C., Weiner, M., Lee, J.H., Duk, L., Na, M.D., 2015. Effects of amyloid and vascular markers on cognitive decline in subcortical vascular dementia. Neurology 85, 1687–1693.

Yu, Q., He, Z., Zubkov, D., Huang, S., Kurochkin, I., Yang, X., Halene, T., Willmitzer, L., Giavalisco, P., Akbarian, S., Khaitovich, P., 2018. Lipidome alterations in human prefrontal cortex during development, aging, and cognitive disorders. Mol. Psychiatry. doi:10.1038/s41380-018-0200-8.

Yun, J.Y., Boedhoe, P.S.W., Vriend, C., Jahanshad, N., Abe, Y., Ameis, S.H., Anticevic, A., Arnold, P.D., Batistuzzo, M.C., Benedetti, F., Beucke, J.C., Bollettini, I., Bose, A., Brem, S., Calvo, A., Cheng, Y., Cho, K.I.K., Ciullo, V., Dallaspezia, S., Denys, D., Feusner, J.D., Fouche, J.P., Giménez, M., Gruner, P., Hibar, D.P., Hoexter, M.Q., Hu, H., Huyser, C., Ikari, K., Kathmann, N., Kaufmann, C., Koch, K.,

Lazaro, L., Lochner, C., Marques, P., Marsh, R., Martínez-Zalacaín, I., Mataix-Cols, D., Menchón, J.M., Minuzzi, L., Morgado, P., Moreira, P., Nakamae, T., Nakao, T., Narayanaswamy, J.C., Nurmi, E.L., O'Neill, J., Piacentini, J., Piras, Fabrizio, Piras, Federica, Reddy, Y.C.J., Sato, J.R., Simpson, H.B., Soreni, N., Soriano-Mas, C., Spalletta, G., Stevens, M.C., Szeszko, P.R., Tolin, D.F., Venkatasubramanian, G., Walitza, S., Wang, Z., van Wingen, G.A., Xu, J., Xu, X., Zhao, Q., Thompson, P.M., Stein, D.J., van den Heuvel, O.A., Kwon, J.S., 2020. Brain structural covariance networks in obsessive-compulsive disorder: a graph analysis from the ENIGMA Consortium. Brain 143, 684–700. doi:10.1093/brain/awaa001.

Zhou, J., Greicius, M.D., Gennatas, E.D., Growdon, M.E., Jang, J.Y., Rabinovici, G.D., Kramer, J.H., Weiner, M., Miller, B.L., Seeley, W.W., 2010. Divergent network connectivity changes in behavioural variant frontotemporal dementia and Alzheimer's disease. Brain 133, 1352–1367 awq075[pii]10.1093/brain/awq075.